NeuroImage: Clinical 9 (2015) 418–429

Contents lists available at ScienceDirect

NeuroImage: Clinical

journal homepage: www.elsevier.com/locate/ynicl

# Joint assessment of white matter integrity, cortical and subcortical atrophy to distinguish AD from behavioral variant FTD: A two-center study

Christiane Möller[a,*], Anne Hafkemeijer[b,d], Yolande A.L. Pijnenburg[a], Serge A.R.B. Rombouts[b,d], Jeroen van der Grond[c], Elise Dopper[a,c,e,f], John van Swieten[e,f], Adriaan Versteeg[g], Petra J.W. Pouwels[h], Frederik Barkhof[g], Philip Scheltens[a], Hugo Vrenken[g,h], Wiesje M. van der Flier[a,i]

[a] Department of Neurology & Alzheimer Center, Neuroscience Campus, VU University Medical Center Amsterdam, Amsterdam, The Netherlands
[b] Institute of Psychology, Leiden University, Leiden, The Netherlands
[c] Department of Radiology, Leiden University Medical Center, Leiden, The Netherlands
[d] Leiden Institute for Brain and Cognition, Leiden University, Leiden, The Netherlands
[e] Department of Clinical Genetics, Neuroscience Campus, VU University Medical Center Amsterdam, Amsterdam, The Netherlands
[f] Department of Neurology, Erasmus Medical Center, Rotterdam, The Netherlands
[g] Department of Radiology & Nuclear Medicine, Neuroscience Campus, VU University Medical Center Amsterdam, Amsterdam, The Netherlands
[h] Department of Physics & Medical Technology, Neuroscience Campus, VU University Medical Center Amsterdam, Amsterdam, The Netherlands
[i] Department of Epidemiology & Biostatistics, Neuroscience Campus, VU University Medical Center Amsterdam, Amsterdam, The Netherlands

ARTICLE INFO

*Article history:*
Received 16 December 2014
Received in revised form 25 August 2015
Accepted 31 August 2015
Available online 9 September 2015

*Keywords:*
Alzheimer's disease
Frontotemporal dementia
Gray matter atrophy
White matter integrity
Discriminant analyses
Diagnosis

ABSTRACT

We investigated the ability of cortical and subcortical gray matter (GM) atrophy in combination with white matter (WM) integrity to distinguish behavioral variant frontotemporal dementia (bvFTD) from Alzheimer's disease (AD) and from controls using voxel-based morphometry, subcortical structure segmentation, and tract-based spatial statistics. To determine which combination of MR markers differentiated the three groups with the highest accuracy, we conducted discriminant function analyses. Adjusted for age, sex and center, both types of dementia had more GM atrophy, lower fractional anisotropy (FA) and higher mean (MD), axial (L1) and radial diffusivity (L23) values than controls. BvFTD patients had more GM atrophy in orbitofrontal and inferior frontal areas than AD patients. In addition, caudate nucleus and nucleus accumbens were smaller in bvFTD than in AD. FA values were lower; MD, L1 and L23 values were higher, especially in frontal areas of the brain for bvFTD compared to AD patients. The combination of cortical GM, hippocampal volume and WM integrity measurements, classified 97–100% of controls, 81–100% of AD and 67–75% of bvFTD patients correctly. Our results suggest that WM integrity measures add complementary information to measures of GM atrophy, thereby improving the classification between AD and bvFTD.

© 2015 The Authors. Published by Elsevier Inc. This is an open access article under the CC BY-NC-ND license (http://creativecommons.org/licenses/by-nc-nd/4.0/).

## 1. Introduction

Alzheimer's disease (AD) and behavioral variant frontotemporal dementia (bvFTD) are the leading causes of young onset dementia (Ratnavalli et al., 2002; Harvey et al., 2003). BvFTD has a very heterogeneous presentation, but is mostly characterized by a marked, progressive decline in personality and/or behavior. Symptoms such as loss of manners or decorum, impulsive actions, apathy and changing of eating behavior are common (Rascovsky et al., 2011). Furthermore, patients often show deficits in cognitive domains of executive functioning, attention and working memory (Rabinovici et al., 2010; Hornberger et al., 2008, 2012). AD is mainly characterized by episodic memory impairment in the initial phase but deficits in visuospatial abilities, executive functioning, language and attention are also common (Nestor et al., 2004; Smits et al., 2011). Clinical diagnostic criteria for bvFTD and AD have been proposed (Rascovsky et al., 2011; McKhann et al., 2011), but the frequent overlap of clinical symptoms associated with AD and bvFTD and heterogeneity within one syndrome pose serious problems in the differential diagnosis (Greicius et al., 2002; Miller et al., 2003; Walker et al., 2005; Harris et al., 2015).

Although the definite diagnosis of both types of dementia is only possible at autopsy, magnetic resonance imaging (MRI), providing measurements of gray matter (GM) atrophy and white matter (WM)

* Corresponding author at: Department of Neurology, Alzheimer Center, VU University Medical Center, PO Box 7057, Amsterdam 1007 MB, The Netherlands. Tel.: +31 20 4440685; fax: +31 20 4440715.
*E-mail address:* crimoe@gmx.net (C. Möller).

http://dx.doi.org/10.1016/j.nicl.2015.08.022
2213-1582/© 2015 The Authors. Published by Elsevier Inc. This is an open access article under the CC BY-NC-ND license (http://creativecommons.org/licenses/by-nc-nd/4.0/).

integrity, have been shown to detect brain changes in an early disease stage. Studies on GM atrophy have shown precuneus, lateral parietal and occipital cortices to be more atrophic in AD than in bvFTD, whereas atrophy of anterior cingulate, anterior insula, subcallosal gyrus, and caudate nucleus was more severe in bvFTD compared to AD (Rabinovici et al., 2007; Du et al., 2007; Looi et al., 2008). However, many scans differ from the predicted patterns of atrophy and overlap between AD and bvFTD is common: GM loss in dorsolateral prefrontal cortex, medial temporal lobes, hippocampus and amygdala is found in both AD and bvFTD and does not help to discriminate between the two disorders (Rabinovici et al., 2007; Munoz-Ruiz et al., 2012; van de Pol et al., 2006; Barnes et al., 2006). Moreover, especially in the beginning of the disease, cortical atrophy may not be visible by eyeballing.

In addition to local GM damage, a decrease of fractional anisotropy (FA) in WM, suggesting WM tract damage has been shown, especially in bvFTD. Previous studies showed that compared to AD, WM integrity was lost in bvFTD especially in the frontal and bilateral temporal regions (Zhang et al., 2009; Chen et al., 2009). Taking into account WM abnormalities holds promise to improve the distinction between AD and bvFTD but only a few studies have been conducted so far (Zhang et al., 2009; Mahoney et al., 2014). Moreover, it is conceivable that the combination of information from GM and WM may help in the discrimination between AD and bvFTD. Most former studies focused on either GM or WM damage however, while only a few investigated the extent to which the loss of WM integrity and GM atrophy are related and how they jointly contribute to the clinical classification of patients (McMillan et al., 2012; Mahoney et al., 2014; Zhang et al., 2011). Generalizability of these findings is limited as in one study patients from the whole FTLD spectrum were compare to AD patients (McMillan et al., 2012) and in other studies the different imaging modalities were only linked to each other but not used for diagnostic discrimination (Mahoney et al., 2014; Zhang et al., 2011).

In this multi-center study we compared patterns of cortical and subcortical GM atrophy and of WM integrity between patients with bvFTD, AD and controls with the ultimate goal to facilitate clinical diagnosis. In addition, we investigated the joint discriminative ability of GM atrophy and WM integrity measurement to distinguish both patient groups from controls and from each other.

## 2. Materials and methods

### 2.1. Patients

In this two center study, we included 39 patients with probable AD and 30 patients with bvFTD, who visited either the Alzheimer Center of the VU University Medical Center (VUMC) (probable AD: n = 23; probable bvFTD: n = 16; possible bvFTD: n = 4) or the Alzheimer Center of the Erasmus University Medical Center Rotterdam (probable AD: n = 16; probable bvFTD: n = 9; possible bvFTD: n = 1). All patients underwent a standardized 1-day assessment including medical history, medical history (dementia, psychiatry, cardiovascular) of first-degree relatives, informant-based history, physical and neurological examination, blood tests, neuropsychological assessment, and MRI of the brain. Diagnoses were made in a multidisciplinary consensus meeting according to the core clinical criteria of the National Institute on Aging and the Alzheimer's Association work group for probable AD (McKhann et al., 1984; McKhann et al., 2011) and according to the clinical diagnostic criteria of FTD for bvFTD (Rascovsky et al., 2011). To minimize center effects, all diagnoses were re-evaluated in a panel including clinicians from both centers. In addition, we included 41 cognitively normal controls (VUMC: n = 23; Rotterdam: n = 18), who were recruited by advertisement in local newspapers. Before inclusion in the present study, controls were screened for memory complaints, family history of dementia, drugs- or alcohol abuse, major psychiatric disorder, and neurological or cerebrovascular diseases. They underwent an assessment including medical history, physical examination, neuropsychological assessment, and MRI of the brain comparable to the work-up of patients.

Inclusion criteria for both cohorts were: (1) availability of a T1-weighted 3-dimensional MRI (3DT1) scan and a set of diffusion weighted imaging (DWI) images designed to allow calculation of the diffusion tensor at 3 T, and (2) age between 50 and 80 years. Exclusion criteria were: (1) large image artifacts (n = 12); (2) failure of imaging analyzing software to process MR scans (n = 6); and (3) gross brain pathology other than atrophy, including severe white matter hyperintensities and/or lacunar infarction in deep gray matter structures. Level of education was rated on a seven-point scale (Verhage, 1964). The study was conducted in accordance with regional research regulations and conformed to the Declaration of Helsinki. The local medical ethics committee of both centers approved the study. All patients gave written informed consent for their clinical and biological data to be used for research purposes.

### 2.2. Neuropsychological assessment

To assess dementia severity we used the Mini-Mental State Examination (MMSE). Cognitive functioning was assessed using a standardized neuropsychological test battery covering five major domains: memory (immediate recall, recognition and delayed recall of Dutch version of the Rey Auditory Verbal Learning Test and total score of Visual Association Test A), language (Visual Association Test picture naming and category fluency (animals: 1 min)), visuospatial functioning (subtest of Visual Object and Space Perception (VOSP) Battery: number location), attention (Trail Making Test part A (TMT A), Digit Span forward, and Letter Digit Substitution Test (LDST)), and executive functioning (Digit Span backwards, Trail Making Test part B (TMT B), letter fluency, and Stroop Color–Word test, card III). For a detailed description of neuropsychological tests see (Smits et al., 2011). For each cognitive task, z-scores were calculated from the raw test scores by the formula $z = (x - \mu) / \sigma$, where $\mu$ is the mean and $\sigma$ is the standard deviation of the subjective complaints group. The value $z = 0$ therefore reflects the average test performance of the subjective complaints group in a given domain. Scores of TMT A, TMT B, and Stroop were inverted by computing $-1 \times$ z-score, because higher scores imply a worse performance. Next, composite z-scores were calculated for each cognitive domain by averaging z-scores. Composite z-scores were calculated when at least one neuropsychological task was available in each cognitive domain.

### 2.3. MR image acquisition and review

Imaging at the VUMC was carried out on a 3 T scanner (Signa HDxt, GE Healthcare, Milwaukee, WI, USA), using an 8-channel head coil with foam padding to restrict head motion. Patients and controls from the Erasmus University Medical Center Rotterdam were all scanned at the Leiden University Medical Center (LUMC). Imaging at LUMC was performed on a 3 T scanner (Achieva, Philips Medical Systems, Best, The Netherlands) using an 8-channel SENSE head coil.

The scan protocol included a whole-brain near-isotropic 3DT1-weighted sequence for cortical and subcortical segmentation. At VUMC this was a fast spoiled gradient echo sequence (FSPGR; repetition time TR 7.8 ms, echo time TE 3 ms, inversion time TI 450 ms, flip angle 12°, 180 sagittal slices, voxel size 0.98 × 0.98 × 1 mm, total scan time 4.57 min). At LUMC this was a turbo field echo sequence (T1TFE; TR 9.8 ms, TE 4.6 ms, flip angle 8°, 140 transversal slices, voxel size 0.88 × 0.88 × 1.2 mm, total scan time 4.57 min). In addition DWI was performed using EPI based sequences. At the VUMC, DWI consisted of five volumes without directional weighting (i.e. $b = 0$ s/mm$^2$) and 30 volumes with noncollinear diffusion gradients (i.e. 30 directions, $b = 1000$ s/mm$^2$) and TR 13,000 ms, TE 87.8 ms, 45 contiguous axial slices of 2.4 mm, voxel size = 2×2 × 2.4 mm, parallel imaging with factor 2, total scan time 7.8 min. At the LUMC DWI consisted of 1 vol

without directional weighting (i.e. b = 0 s/mm$^2$) and 60 volumes with noncollinear diffusion gradients (i.e. 60 directions, b = 1000 s/mm$^2$) and TR 8250 ms, TE 80 ms, 70 axial slices, voxel size = 2×2 × 2 mm, parallel imaging with factor 2, total scan time 9 min.

In addition, the MRI protocol included a 3D Fluid Attenuated Inversion Recovery (FLAIR) sequence, dual-echo T2-weighted sequence, and susceptibility weighted imaging (SWI) which were reviewed for brain pathology other than atrophy by an experienced radiologist.

### 2.4. Gray matter volume

DICOM images of the 3DT1-weighted sequence were corrected for gradient nonlinearity distortions and converted to Nifti format, after which the image origin was automatically placed approximately on the anterior commissure using a linear registration procedure. The structural 3DT1 images were then analyzed using the voxel-based morphometry toolbox (VBM8; version 435; University of Jena, Department of Psychiatry) in Statistical Parametric Mapping (SPM8; Functional Imaging Laboratory, University College London, London, UK) implemented in MATLAB 7.12 (MathWorks, Natick, MA). In the first module of the VBM8 Toolbox ("Estimate and Write") the 3DT1 images are normalized to MNI space and segmented into GM, WM and cerebrospinal fluid (CSF). We used the default settings, except for the clean-up, where we used the light clean-up option to remove any remaining non-brain tissue, as advised in the VBM8 tutorial. Tissue classes were normalized in alignment with the template with the 'non-linear only' option which allows comparing the absolute amount of tissue corrected for individual brain size. The correction is applied directly to the data, which makes a head-size correction to the statistical model redundant. Subsequently, all segmentations were checked with the second and third module of the VBM8 Toolbox ("Display one slice for all images" and "Check sample homogeneity using covariance") and by a one-by-one visual check. In the fourth module, images were smoothed using an 8 mm full width at half maximum (FWHM) isotropic Gaussian kernel.

Voxelwise statistical comparisons between groups were made to localize GM differences by means of a full factorial design with diagnosis (AD, bvFTD, controls) as factor with independent levels with unequal variance, using absolute threshold masking with a threshold of 0.1 and implicit masking. Age, sex and center were entered as covariates. Post hoc, we compared AD with controls, bvFTD with controls, and AD with bvFTD. The threshold for significance in all VBM analyses was set to $p < 0.05$ with family wise error correction (FWE) at the voxel level and an extent threshold of 0 voxel.

### 2.5. Volumes of deep gray matter (DGM) structures

The algorithm FIRST (FMRIB's integrated registration and segmentation tool) (Patenaude et al., 2011) was applied to estimate left and right volumes of five DGM structures: thalamus, caudate nucleus, putamen, globus pallidus, and nucleus accumbens, and two medial temporal lobe (MTL) structures: hippocampus and amygdala. Left and right volumes were summed to obtain total volume for each structure. FIRST is integrated in FMRIB's software library (FSL 4.15) (Jenkinson et al., 2012) and performed both registration and segmentation of the above mentioned anatomical structures. A two-stage linear registration was performed to achieve a more robust and accurate pre-alignment of the seven structures. During the first-stage registration, the 3DT1 images were registered linearly to a common space based on the Montreal Neurological Institute (MNI) 152 template with 1 × 1 × 1 mm resolution using 12 degrees of freedom. After registration, a second stage registration using a subcortical mask or weighting image, defined in MNI space, was performed to improve registration for the seven structures. Both stages used 12 degrees of freedom. This 2-stage registration was followed by segmentation based on shape models and voxel intensities. Volumes of the seven structures were extracted in native space, taking into account the transformations matrices during registration. The final step was a boundary correction based on local signal intensities. All registrations and segmentations were visually checked for errors.

To correct the volumes of the seven structures for head size we used a volumetric scaling factor (VSF) derived from the normalization transform matrix from SIENAX (Structural Image Evaluation using Normalization of Atrophy Cross-sectional) (Smith et al., 2002), also part of FSL. In short, SIENAX extracted skull and brain from the 3DT1 input whole-head image. In our study, brain extraction was performed using optimized parameters (Popescu et al., 2012). These were then used to register the subject's brain and skull image to standard space brain and skull (derived from MNI152 template) to estimate the scaling factor (VSF) between the subject's image and standard space. Normalization for head size differences was done by multiplying the raw volumes of the seven structures by the VSF. Next to the VSF, we also obtained brain tissue volumes of GM and WM (Zhang et al., 2001). Total volumes of the seven structures and volumes of GM and WM, and VSF were transferred to SPSS for further statistical analyses.

### 2.6. White matter integrity

All preprocessing steps of the DWI images were performed using FSL (Jenkinson et al., 2012; Smith et al., 2004), including motion- and eddy-current correction on images and gradient-vectors, followed by diffusion tensor fitting. Fractional anisotropy (FA), mean diffusivity (MD), axial diffusivity (L1; largest eigenvalue), and radial diffusivity (L23; average of the two smallest eigenvalues L2 and L3) were derived for each voxel. Each subject's FA image was used to calculate nonlinear registration parameters to the FMRIB58_FA brain, which were then applied to all four parameter images. The registered FA images were averaged into a mean FA image, which was skeletonized for tract-based spatial statistics (TBSS) (Smith et al., 2006). The skeleton was thresholded at 0.2 to include only WM and used for TBSS statistics in all diffusion parameters. Each subject's aligned FA data was then projected onto this skeleton and the resulting data fed into voxelwise cross-subject statistics. The projection parameters for each voxel were then also applied to the MD, L1 and L23 data to create skeletonized data in standard space for each subject. Differences in FA, MD, L1 and L23 between controls, AD and bvFTD patients were analyzed in a voxelwise fashion using FSL's randomize with 5000 permutations and age, sex and center as covariates. A family wise error (FWE) corrected Threshold-Free Cluster Enhancement (TFCE) significance level of $p < 0.05$ was used to correct for multiple comparisons.

### 2.7. Extraction of regions of interest (ROI)

As a next step, we extracted ROIs from the VBM and TBSS group analyses, to be able to combine the most promising MR markers in one statistical model.

Gray matter ROIs (VBM): We extracted all significant voxels from the resulting T-maps from the comparisons AD < controls, bvFTD < controls, and bvFTD < AD from the VBM analyses. This resulted in three GM ROIs: 'GM ROI AD < Controls', 'GM ROI bvFTD < Controls', 'GM ROI bvFTD < AD'. This was done by merging the normalized modulated GM segments of all subjects into a 4D file. The T-maps of all contrasts were thresholded at $p < 0.05$ (FWE corrected) and binarized. We then calculated the GM volume of each of the three ROIs and transferred it to SPSS for further analyses.

White matter integrity ROIs (TBSS): We extracted all significant voxels (TFCE, FWE corrected $p < 0.05$) from the statistical contrast image from the comparisons AD < controls, bvFTD < controls, and bvFTD < AD. This resulted in three FA ROIs: 'FA ROI AD < Controls', 'FA ROI bvFTD < Controls', 'FA ROI bvFTD < AD'. We then calculated the mean FA in each of the three ROIs. The same was done for MD, L1 and L23, resulting in three ROIs per diffusivity measurement. We transferred mean FA, MD, L1 and L23 of all ROIs to SPSS for further analysis.

### 2.8. Statistical analysis

SPSS version 20.0 for Windows was used for statistical analysis. Differences between groups for demographics and cognition were assessed using univariate analysis of variance (ANOVA) (age, VSF, NBV), Kruskal–Wallis tests (level of education, MMSE, GDS, CDR, composite cognitive domain z-scores) and $\chi^2$ test (sex, center, history of dementia, psychiatry, cardio-vascular events in first-degree relative).

Multivariate analysis of variance (MANOVA) was used to compare total head-size corrected volumes of MTL and DGM structures (dependent variables) between the different diagnostic groups (between-subjects factor) with Bonferroni adjusted post hoc tests. Age, sex and center were used as covariates.

To determine which combination of MR markers based on VBM, DGM structures and TBSS measurements differentiated the three patient groups with the highest accuracy, we conducted a discriminant function analysis with leave-one-out cross validation. As predictors we entered the following variables: 'GM ROI AD < Controls', 'GM ROI bvFTD < Controls', 'GM ROI bvFTD < AD'; total head-size corrected volumes of hippocampus, thalamus, caudate nucleus, putamen and nucleus accumbens (as these structures significantly differed between the groups); 'FA ROI AD < Controls', 'FA ROI bvFTD < Controls', 'FA ROI bvFTD < AD'; as well as sex, age, and center. Because of colinearity we performed another discriminant function analyses with the other diffusion parameters L1 and L23 instead of FA. In this discriminant function we used the following variables as predictors: 'GM ROI AD < Controls', 'GM ROI bvFTD < Controls', 'GM ROI bvFTD < AD'; total head-size corrected volumes of hippocampus, thalamus, caudate nucleus, putamen and nucleus accumbens; 'L1 ROI AD > controls', 'L1 ROI bvFTD > controls', 'L1 ROI bvFTD > AD', 'L23 ROI AD > controls', 'L23 ROI bvFTD > controls', 'L23 ROI bvFTD > AD'; as well as sex, age, and center.

In general, a discriminant analysis creates k-1 linear combinations (discriminant functions) of the entered predictor variables which provides the best discrimination between the groups (k). To identify the most optimal combination of variables for best discrimination, stepwise forward analysis was used with a decision scheme based on the F-value of Wilk's lambda (entry: 3.84; removal: 2.71). Statistical significance for all analyses was set at $p < 0.05$.

## 3. Results

### 3.1. Demographics

Demographic and cognitive data for all patients (AD: $n = 32$; bvFTD: $n = 24$) and controls ($n = 37$) fulfilling inclusion criteria are summarized in Table 1. AD patients were older than controls ($p < 0.001$); there were no differences in gender distribution or education. Compared to controls and AD, bvFTD patients had less first degree relative with dementia. Compared to controls, AD and bvFTD performed worse on all cognitive domains, except on visuospatial functioning. Compared to bvFTD patients, AD patients performed worse on memory and attention. Both dementia groups had smaller normalized brain volumes than controls ($p < 0.001$). AD patients had lower MMSE scores than both other groups ($p < 0.05$). CDR and GDS scores were lowest in controls ($p < 0.001$) but did not differ between the two dementia groups.

### 3.2. Gray matter volume

The full factorial design showed main effects of diagnosis (Fig. 1). Post hoc comparisons showed that compared to controls, AD patients showed a reduction of GM in superior and middle temporal gyrus, parahippocampal gyrus, hippocampus, posterior cingulate, mid cingulum, cuneus, precuneus, occipital lobe, superior and inferior parietal lobe and inferior frontal gyrus ($p < 0.05$, FWE corrected). BvFTD patients had less GM compared to controls in superior, middle, and inferior frontal gyrus, orbito-frontal gyrus, insular, temporal gyrus, parahippocampal gyrus and hippocampus. Controls did not show any regions with less GM than AD or bvFTD ($p < 0.05$, FWE corrected). Compared to AD patients, bvFTD patients had less GM matter in left inferior and medial frontal gyrus, in right inferior frontal gyrus, and in orbitofrontal gyrus ($p < 0.05$, FWE corrected). AD patients did not show any regions of significantly reduced GM compared to bvFTD patients. For comparisons between patient groups we also explored the results at a non-corrected $p = 0.001$ level (figure in supplementary materials): Compared to AD patients, bvFTD patients showed less GM in orbitofrontal, inferior frontal, medial frontal lobe, temporal pole, fusiform gyrus and anterior cingulate. Compared to bvFTD patients, AD patients showed less GM in precuneus, posterior cingulate, occipital lobe, angular gyrus and inferior parietal lobe.

**Table 1**
Demographics.

| | Controls | AD | bvFTD |
|---|---|---|---|
| N | 37 | 32 | 24 |
| Age, years | 60.4 ± 6.2 | 66.7 ± 7.7[a] | 63.2 ± 7.5 |
| Sex, females (n, %) | 16 (43%) | 12 (38%) | 6 (25%) |
| Center, VUMC | 22 (60%) | 22 (69%) | 18 (75%) |
| Level of education | 5.6 ± 1.0 | 5.0 ± 1.4 | 4.8 ± 1.6 |
| Duration of symptoms (months) | – | 40.2 ± 4.6 | 50.0 ± 8.9 |
| MMSE | 28.9 ± 1.4 | 23.2 ± 3.1[a] | 25.1 ± 3.1[a,b] |
| CDR | 0 ± 0 | 0.8 ± 0.3[a] | 0.8 ± 0.3[a] |
| GDS | 1.1 ± 1.3 | 3.0 ± 3.1[a] | 3.8 ± 2.9[a] |
| History of dementia (n, %) | 24 (65%) | 19 (61%) | 8 (33%)[a,b] |
| History of Psychiatry (n, %) | 3 (14%) | 2 (9%) | 5 (28%) |
| History of cardiovascular events (n, %) | 8 (36%) | 14 (61%) | 9 (47%) |
| Memory | 0.0 ± 0.7 | −5.1 ± 3.2[a] | −2.4 ± 1.9[a,b] |
| Language | −0.1 ± 0.9 | −1.2 ± 1.6[a] | −1.7 ± 1.5[a] |
| Visuospatial functioning | 0.0 ± 1.0 | −1.0 ± 1.9 | −0.3 ± 1.0 |
| Attention | −0.1 ± 0.8 | −2.3 ± 1.9[a] | −1.5 ± 1.8[a,b] |
| Executive functioning | 0.0 ± 0.8 | −3.3 ± 2.5[a] | −2.2 ± 2.3[a] |
| NBV ($cm^3$) | 1493.7 ± 64.1 | 1395.2 ± 76.2[a] | 1394.81 ± 87.6[a] |
| VSF | 1.3 ± 0.1 | 1.3 ± 0.1 | 1.3 ± 0.1 |

Values presented as mean ± standard deviation or n%. Level of education is determined according to the Verhage-system. Differences between groups for demographics were assessed using ANOVA, Kruskall–Wallis tests and $\chi^2$ tests, where appropriate.
Abbreviations: MMSE: Mini-Mental State Examination; CDR: Dementia Rating Scale; GDS: Geriatric Depression Scale; NBV: normalized brain volume; VSF: volumetric scaling factor. Cognitive composite z-domains were calculated of the available z-scores of each test by the MEAN function in SPSS.
[a] Different from controls ($p < 0.05$).
[b] Different from AD ($p < 0.05$).

### 3.3. Volumes of deep gray matter structures

Normalized volumes of MTL and DGM structures are summarized in Table 2. MANOVA adjusted for age, sex and center revealed group differences in hippocampus, thalamus, caudate nucleus, putamen and nucleus accumbens (Fig. 2). Post hoc tests showed that nucleus accumbens and caudate nucleus volume discriminated all groups, with bvFTD having most severe atrophy. Hippocampus and thalamus discriminated dementia patients from controls. bvFTD patients had smaller putaminal volumes than controls.

### 3.4. White matter integrity

Fig. 3 shows the mean skeleton with significant regions in FA, MD, L1 and L23 for different group comparisons. Compared with controls, AD patients showed widespread patterns of lower FA values, incorporating 44% of the WM skeleton voxels, in areas including the fornix, corpus callosum, forceps minor, thalamus, posterior thalamic radiation, superior and inferior longitudinal fasciculus. Furthermore, they had higher MD values in 36% of the WM skeleton voxels including the

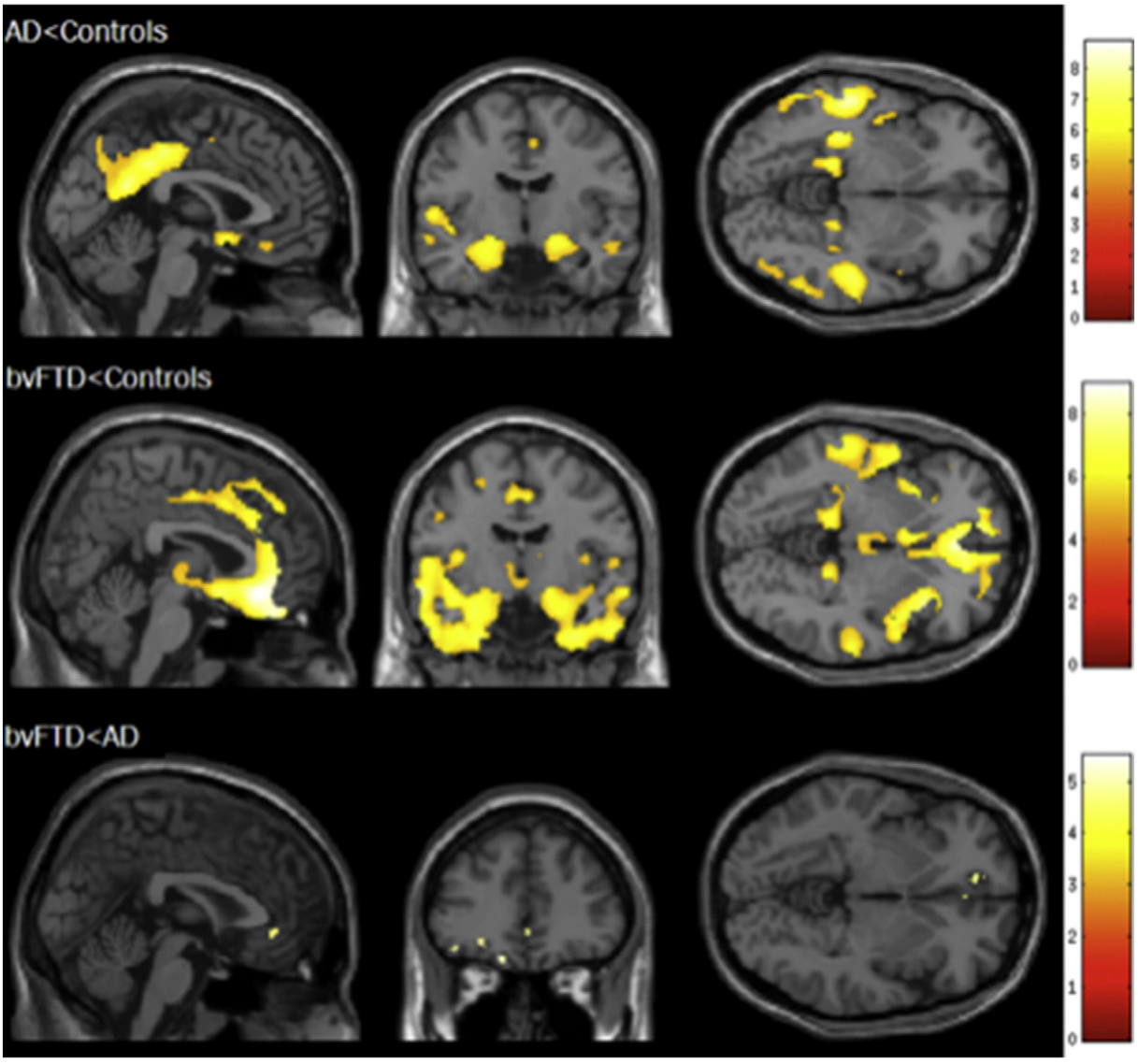


**Fig. 1.** VBM voxel-wise statistical analysis of GM reductions between groups. Figures are displayed with a threshold of $p < 0.05$, FWE corrected. Brighter colors indicate higher t values.

fornix, corpus callosum, forceps minor and forceps major, higher L1 values in 23% of the WM skeleton voxels including the corpus callosum, the corticospinal tract and inferior longitudinal fasciculus, and higher L23 values in 42% of the WM skeleton voxels including the forceps major, inferior fronto-occipital fasciculus, inferior and superior longitudinal fasciculus and the corpus callosum compared with controls.

Compared to controls, bvFTD patients showed widespread patterns of lower FA values in 58% of the investigated WM voxels throughout the whole brain, in areas including the fornix, corpus callosum, forceps minor, thalamus, anterior thalamic radiation, superior and inferior longitudinal fasciculus and inferior fronto-occipital fasciculus. Furthermore, they had higher MD values in 55% of the investigated WM voxels including the inferior fronto-occipital fasciculus, uncinate

**Table 2**
Total volumes ($cm^3$) of MTL and DGM structures, corrected for head size.

| | Controls | AD | bvFTD | | Ctrl > AD | | Ctrl > bvFTD | | AD > bvFTD | |
|---|---|---|---|---|---|---|---|---|---|---|
| | | | | p | Mean difference | p | Mean difference | p | Mean difference | p |
| Hippocampus | 10.3 ± 1.0 | 8.4 ± 1.5[a] | 8.3 ± 1.4[a] | <***0.001*** | 1.707 | <***0.001*** | 1.847 | <***0.001*** | 0.140 | 1.000 |
| Amygdala | 3.6 ± 0.6 | 3.4 ± 1.5 | 3.3 ± 0.6 | 0.082 | | | | | | |
| Thalamus | 19.8 ± 1.7 | 18.1 ± 2.0[a] | 18.1 ± 1.7[a] | <***0.001*** | 1.227 | ***0.006*** | 1.689 | <***0.001*** | 0.461 | 0.793 |
| Caudate nucleus | 9.0 ± 0.8 | 8.7 ± 0.9 | 8.0 ± 1.1[a,b] | <***0.001*** | 0.128 | 1.000 | 0.978 | <***0.001*** | 0.850 | ***0.002*** |
| Putamen | 12.3 ± 1.1 | 11.2 ± 1.4 | 11.1 ± 1.4[a] | ***0.001*** | 0.231 | 0.631 | 1.118 | ***0.001*** | 0.485 | 0.364 |
| Globus pallidus | 4.8 ± 0.7 | 4.6 ± 0.8 | 4.3 ± 0.8 | 0.071 | | | | | | |
| Nucleus accumbens | 1.1 ± 0.2 | 0.9 ± 0.3[a] | 0.8 ± 0.2[a,b] | <***0.001*** | 0.143 | ***0.031*** | 0.331 | <***0.001*** | 0.187 | ***0.005*** |

Values are presented as mean $cm^3$ ± standard deviation. Comparisons are Bonferroni corrected with age, sex and center as covariates.
[a] Different from controls.
[b] Different from AD.

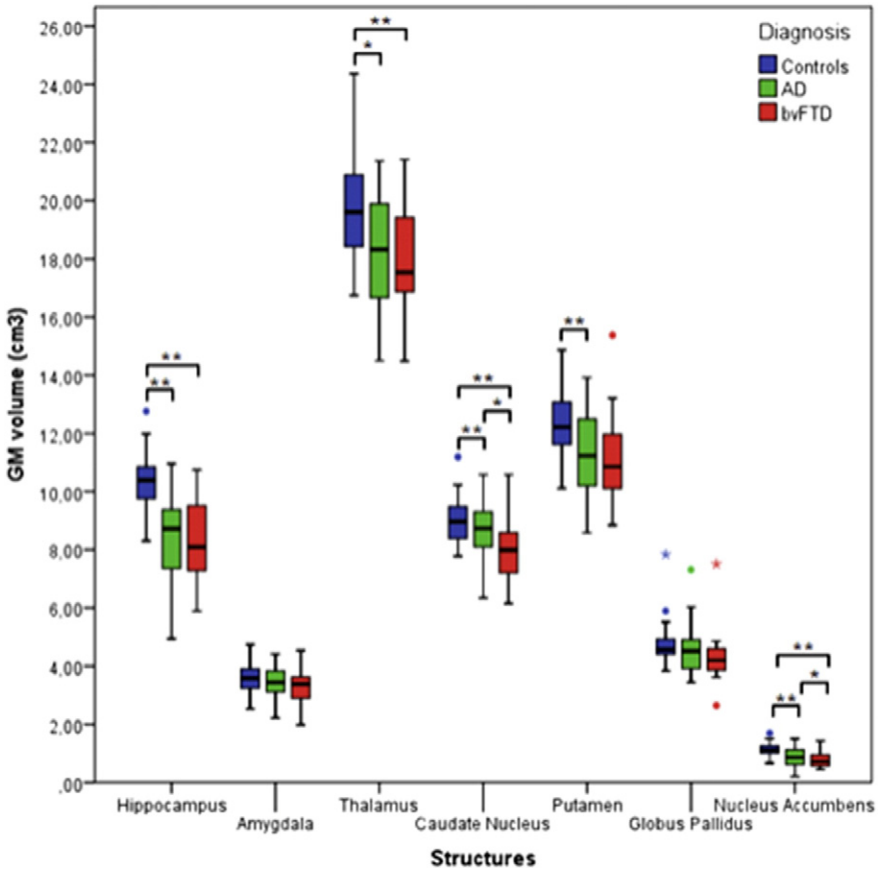


**Fig. 2.** Boxplot of volumes ($cm^3$) of MTL and DGM structures. $^{**}p \leq 0.001$, $^{*}p < 0.05$.

fasciculus and the forceps minor. They had higher L1 values in 39% of the WM skeleton voxels including the inferior fronto-occipital fasciculus, inferior longitudinal fasciculus, corticospinal tract and corpus callosum, and higher L23 values in 62% of the investigated WM voxels in the inferior and superior longitudinal fasciculus, corticospinal tract, corpus callosum, fornix, inferior fronto-occipital fasciculus and the anterior thalamic radiation compared to controls.

In direct comparison between the two dementia groups, bvFTD patients had lower FA values in 17% of the investigated voxels, solely located in the frontal parts of the brain, like the rostrum and the genu of the corpus callosum, forceps minor, anterior part of the internal and external capsule, anterior parts of the fronto-occipital fasciculus and superior longitudinal fasciculus. Furthermore, bvFTD patients had higher MD values in 21% and higher radial diffusivity values in 23% of the investigated WM voxels including forceps minor, uncinate fasciculus, inferior fronto-occipital fasciculus and anterior thalamic radiation, higher axial diffusivity values in 14% of the investigated WM voxels including inferior fronto-occipital fasciculus, uncinate fasciculus and forceps minor compared to AD patients. AD patients had no areas of reduced diffusivity or increased fractional anisotropy compared to bvFTD.

### *3.5. Extraction of regions of interest (ROI)*

In Fig. 4 the GM, FA, MD, L1 and L23 ROIs are depicted. The ROIs represent all significant voxels from a two-group-comparison. In Table 3 compositions of the different ROIs are summarized.

### *3.6. Predictive value of GM volume, volumes of DGM structures, and white matter integrity*

Subsequently, we used discriminant analysis to identify the combination of MR-markers providing optimal classification. Using stepwise forward method, the first discriminant analysis selected the following predictors: (1) GM ROI AD < Controls; (2) hippocampal volume; (3) volume of putamen; (4) FA ROI AD < Controls; (5) FA ROI bvFTD < Controls; (6) center; (7) age; and (8) sex. The two resulting discriminant functions had a Wilk's lambda of 0.082 ($p \leq 0.001$) and 0.388 ($p \leq 0.001$). Fig. 5a shows the projection plot of the two canonical discriminant functions for discrimination of the three groups. Discriminant function 1 discriminated AD from bvFTD and controls. Discriminant function 2 discriminated bvFTD from AD and controls. The loadings of the individual predictors for each function are shown in Table 4a. GM ROI AD < Controls had the highest loading on discriminant function 1. Discriminant function 2 was primarily composed of the variables FA ROI bvFTD < Controls, hippocampal volume, FA ROI AD < Controls, and GM ROI AD < Controls. Cross-validation successfully classified 91.4% of all cases correctly, with correct classification of 100% of controls, 100% of AD patients, and 66.7% of bvFTD patients.

The second discriminant analysis selected the following predictors: (1) GM ROI AD < Controls; (2) GM bvFTD < AD; (3) L1 ROI AD > Controls; (4) L1 ROI bvFTD > Controls; and (5) L1 ROI bvFTD > AD. The two resulting discriminant functions had a Wilk's lambda of 0.134 ($p \leq 0.001$) and 0.437 ($p \leq 0.001$). Fig. 5b shows the projection plot of the two canonical discriminant functions for discrimination of the three groups. Discriminant function 1 discriminated AD from bvFTD and controls. Discriminant function 2 discriminated bvFTD from AD and controls. The loadings of the individual predictors for each function are shown in Table 4b. GM ROI AD < Controls and L1 ROI AD < Controls had the highest loadings on discriminant function 1. Discriminant function 2 was primarily composed of GM ROI bvFTD < AD, L1 ROI bvFTD < AD, L1 ROI bvFTD > Controls, GM ROI AD < Controls, and L1 ROI AD > Controls. Cross-validation successfully classified 86% of all cases correctly, with correct classification of 97.3% of controls, 81.3% of AD patients, and 75% of bvFTD patients.

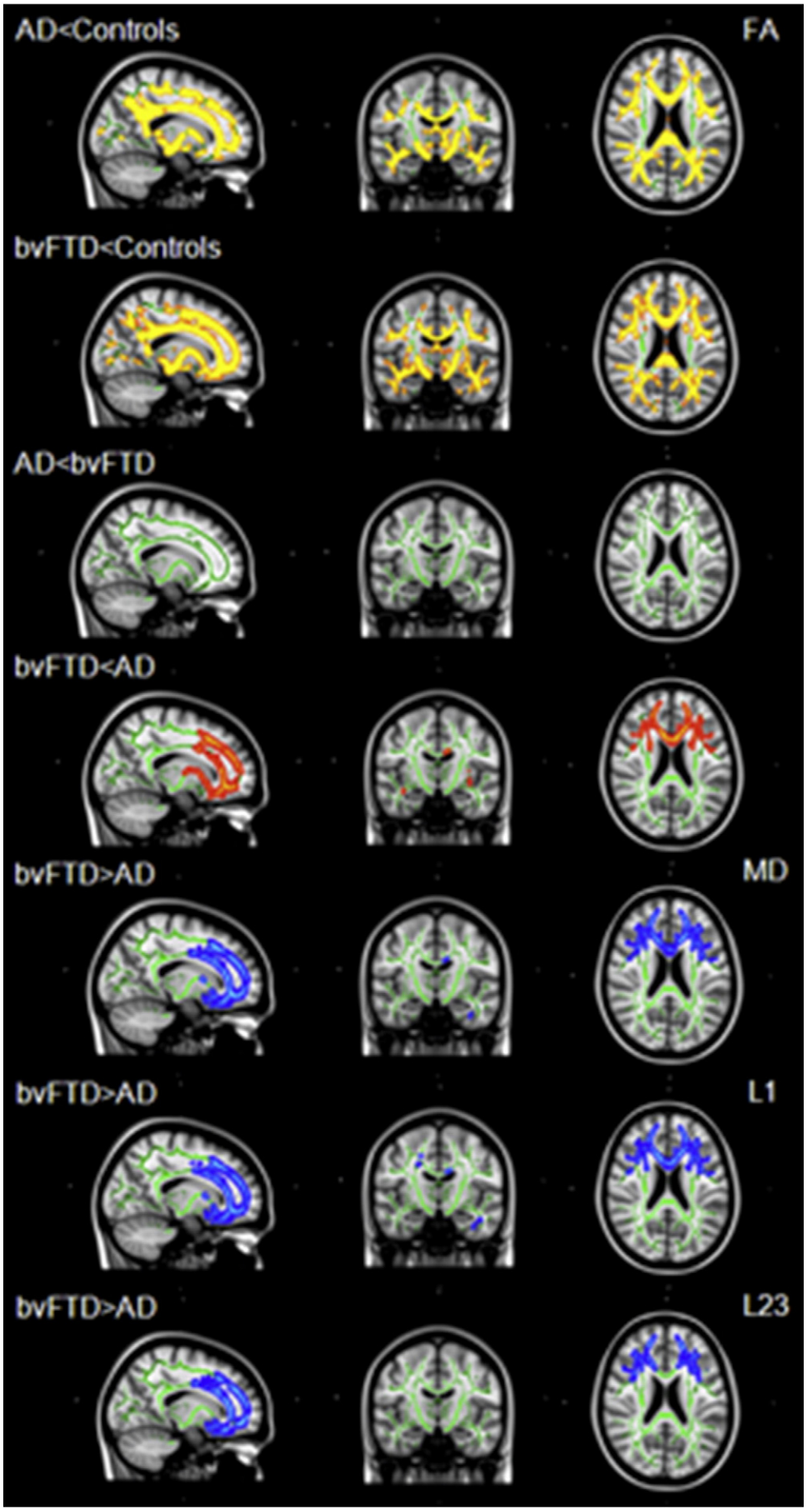
AD<Controls
FA
bvFTD<Controls
AD<bvFTD
bvFTD<AD
bvFTD>AD
MD
bvFTD>AD
L1
bvFTD>AD
L23

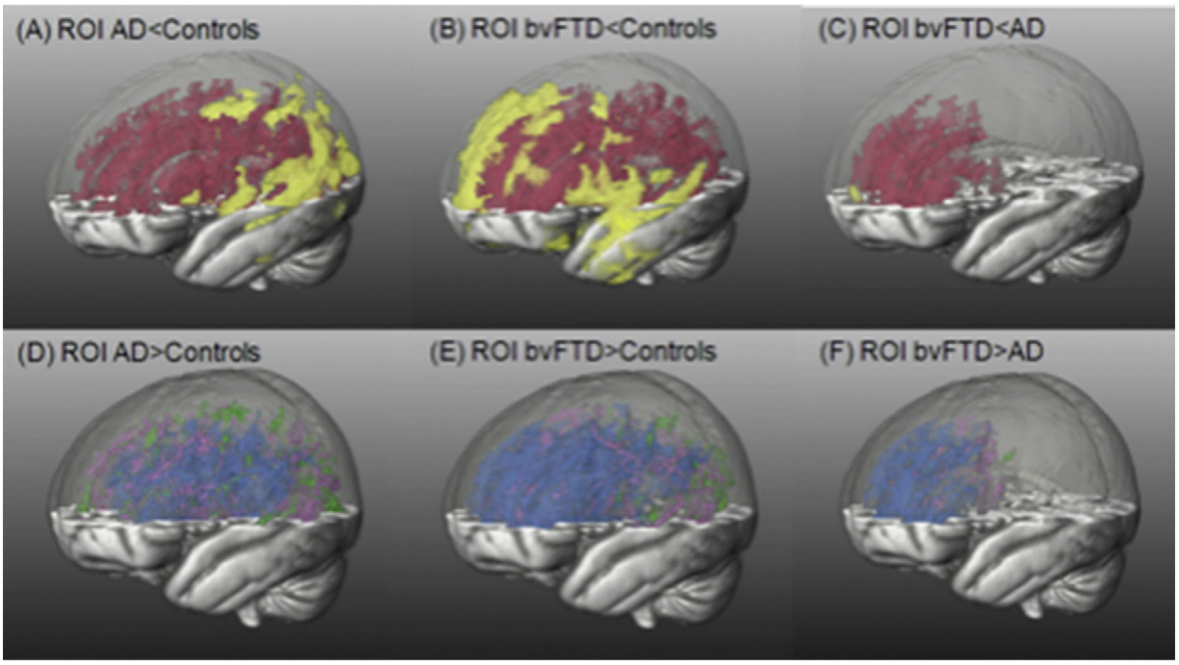


**Fig. 4.** Composition of GM, FA, MD, L1 and L23 ROIs per contrast. Figures A–C show ROIs of reduced GM and lower FA. Figures D–F show ROIs of increased MD, L1 and L23. (A) GM and FA ROIs AD < controls: All significant voxels ($p < 0.05$, FWE and FWE TFCE corrected) where AD patients had less GM (yellow) and lower FA values (red) compared to controls.(B) GM and FA ROIs bvFTD < controls: All significant voxels ($p < 0.05$, FWE and TFCE corrected) where bvFTD patients had less GM (yellow) and lower FA values (red) compared to controls.(C) GM and FA ROIs bvFTD < AD: All significant voxels ($p < 0.05$, FWE and FWE TFCE corrected) where bvFTD patients had less GM (yellow) and lower FA values (red) compared to AD patients.(D) MD, L1 andL23 ROIs AD > controls: All significant areas ($p < 0.05$, FWE TFCE corrected) from the TBSS group comparisons where AD patients had higher MD (pink), higher L1 (blue) and higher L23 (green) values compared to controls.(E) MD, L1 and L23 ROIs bvFTD > controls: All significant areas ($p < 0.05$, FWE TFCE corrected) from the TBSS group comparisons where bvFTD patients had higher MD (pink), higher L1 (blue) and higher L23 (green) values compared to controls.(F) MD, L1 and L23 ROIs bvFTD > AD: All significant areas ($p < 0.05$, FWE TFCE corrected) from the TBSS group comparisons where bvFTD patients had higher MD (pink), higher L1 (blue) and higher L23 (green) values compared to AD patients.

**Table 3**
Composition of each ROI per group comparison for GM, FA, MD, L1 and L23 measurement.

| Measurement | Group comparison | Brain regions incorporated in ROI |
|---|---|---|
| GM | AD < Ctrl | Temporal gyrus, posterior cingulate, cuneus, precuneus, inferior & superior parietal lobe, inferior frontal gyrus |
| FA | | Fornix, corpus callosum, forceps minor, thalamus, posterior thalamic radiation, superior & inferior longitudinal fasciculus |
| GM | BvFTD < Ctrl | Frontal gyrus, orbito-frontal gyrus, insula, temporal gyrus |
| FA | | Fornix, corpus callosum, forceps minor, thalamus, anterior thalamic radiation, superior & inferior longitudinal fasciculus, inferior fronto-occipital fasciculus |
| GM | BvFTD < AD | Left inferior & medial frontal gyrus, right inferior frontal gyrus, orbito-frontal gyrus |
| FA | | Rostrum & genu of corpus callosum, forceps minor, anterior part of internal & external capsule, anterior parts of fronto-occipital fasciculus, superior longitudinal fasciculus |
| MD | AD > Ctrl | Fornix, corpus callosum, forceps minor, forceps major |
| L1 | | Corpus callosum, corticospinal tract, inferior longitudinal fasciculus |
| L23 | | Forceps major, inferior fronto-occipital fasciculus, inferior & superior longitudinal fasciculus, corpus callosum |
| MD | BvFTD > Ctrl | Inferior fronto-occipital fasciculus, uncinate fasciculus, forceps minor |
| L1 | | Inferior fronto-occipital fasciculus, inferior longitudinal fasciculus, corticospinal tract, corpus callosum |
| L23 | | Inferior & superior longitudinal fasciculus, corticospinal tract, corpus callosum, fornix, inferior fronto-occipital fasciculus, anterior thalamic radiation |
| MD | BvFTD > AD | Forceps minor, uncinate fasciculus, inferior fronto-occipital fasciculus, anterior thalamic radiation |
| L1 | | Inferior fronto-occipital fasciculus, uncinate fasciculus, forceps minor |
| L23 | | Forceps minor, uncinate fasciculus, inferior fronto-occipital fasciculus, anterior thalamic radiation |

Brain regions are listed where significant voxels were detected from the group comparisons per measurement.

## 4. Discussion

The main finding of this study is that there are GM and clear WM differences between AD and bvFTD which both independently contributed to the classification of both types of dementia. Despite a comparable disease stage, bvFTD patients had more atrophy in orbitofrontal and inferior frontal areas, caudate nucleus and nucleus accumbens than AD patients. Furthermore, they had more severe loss of FA, higher MD, L1 and L23 values, especially in the frontal areas. Combination of modalities led to 86–91.4% correct classification of patients. GM contributed most to distinguishing AD patients from controls and bvFTD patients, while WM integrity measurements, especially L1, contributed to distinguish bvFTD from controls and AD.

A large number of studies investigated the differences between controls and AD or bvFTD patients with regard to either GM or WM pathology. Their results are in line with the current study showing GM

**Fig. 3.** TBSS voxelwise statistics displaying areas of white matter skeleton (green) with lower FA (red-yellow) and higher MD, L1, L23 (blue–light-blue) values, overlaid on the MNI-standard brain. Significance level of $p < 0.05$ with correction for multiple comparisons was used. Skeletonized results are thickened to enhance figure clarity. These thickened results are based on the original p-maps.

atrophy of medial temporal lobe structures and temporoparietal lobes in AD (Whitwell et al., 2011; Möller et al., 2013; Frisoni et al., 2002) and atrophy of orbitofrontal, anterior cingulate, insula, lateral temporal cortices, and caudate nucleus in bvFTD (Rabinovici and Miller, 2010; Hornberger et al., 2011; Couto et al., 2013; Looi et al., 2012). DTI studies on AD reported a rather consistent pattern of FA reductions in widely distributed WM tracts exceeding MTL regions (Scola et al., 2010; Agosta et al., 2011; Salat et al., 2010). In patients with bvFTD significant FA reductions in the superior and inferior longitudinal fasciculus, as well as additional FA decreases in the uncinate fasciculus and the genu of the corpus callosum have been reported (Borroni et al., 2007; Matsuo et al., 2008).

To determine whether GM atrophy or WM integrity have potential diagnostic use, a direct comparison between AD and bvFTD is more important than the comparison with a control group. With respect to GM atrophy, precuneus, lateral parietal and occipital cortices have been shown to be more atrophic in AD than in bvFTD, whereas atrophy of anterior cingulate, anterior insula, subcallosal gyrus, and caudate nucleus are more atrophic in bvFTD compared to AD (Rabinovici et al., 2007; Du et al., 2007; Looi et al., 2008). In our study, we did not find any areas which are more atrophic in AD compared to bvFTD. This could be explained by the strict FWE-corrected VBM approach, as we found less GM in posterior brain regions in AD patients when not applying the multiple comparisons correction. These results are in line with another study not applying multiple comparisons correction (Rabinovici et al., 2007). Another explanation that we did not find any GM reductions in AD could be that our patients are included in an early disease stage, with relatively higher MMSE scores compared to another study (Du et al., 2007). Nevertheless, patterns of GM atrophy often overlap, as there are numerous regions of GM loss which are found in both AD and bvFTD (Rabinovici et al., 2007; Munoz-Ruiz et al., 2012; van de Pol et al., 2006; Barnes et al., 2006). The few existing DTI studies demonstrated WM alterations in FTD compared to AD, including more widespread FA reductions in the frontal, anterior temporal, anterior corpus callosum, inferior fronto-occipital fasciculus and bilateral anterior cingulum (Zhang et al., 2009, 2011; Hornberger et al., 2011; Avants et al., 2010; McMillan et al., 2012). One of these studies also investigated the MD, L1 and L23 differences between FTD and AD and found increased L1 and L23 values in FTD compared to AD (Zhang et al., 2009). Our study is in line with these previous studies, failing to observe reduced FA and increased MD, L1 and/or L23 in AD relative to bvFTD. The same is seen in the DGM structures, where bvFTD patients have more subcortical brain damage compared to AD patients but not the other way around (Looi et al., 2008, 2009; Halabi et al., 2013). The combination of different imaging analysis methods suggests that the non-cortical parts of the brain play an important role in bvFTD. Networks in bvFTD, consisting of white matter and deep gray matter structures, may be different compared to the cortical networks in AD. Indeed, studies of functional connectivity show more functional network connectivity in FTD compared to controls and AD (Filippi et al., 2013; Zhou et al., 2010). Studies using multimodel network analyses should focus on this topic in future studies.

We attempted to combine GM and WM measures to increase the discrimination of patient groups and showed that next to GM atrophy, WM integrity measures helped in distinguishing AD from bvFTD. A few earlier studies have combined WM and GM information with the objective to better discriminate between AD and bvFTD. They found that FTD patients exhibited more WM damage than AD patients in an early stage of the disease suggesting that measuring of WM damage add up in the discrimination between these two dementias (Zhang et al., 2011; Mahoney et al., 2014). Another study only linked the two imaging modalities and support the idea of a network disease in FTD but did not examine diagnostic value of GM and WM (Avants et al., 2010). Only two studies actually used a multimodal combination of WM and GM. In one study they achieved a classification with 87% sensitivity and 83% specificity between AD and bvFTD (McMillan et al., 2012). In another study they developed a new metric which gives a measure of the amount of WM connectivity disruption for a GM region and showed classification rates were 8–13% higher when adding WM measurements to GM measurements (Kuceyeski et al., 2012).

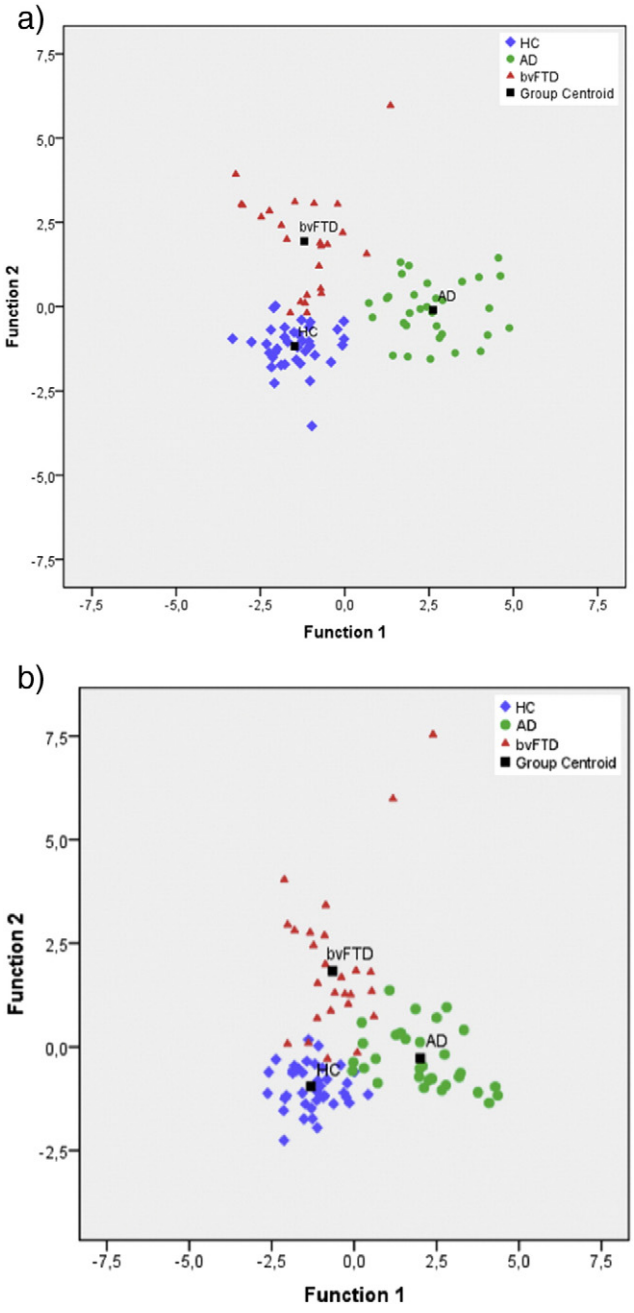


**Fig. 5.** Projection plot of canonical discriminant functions for discrimination of healthy controls, AD and bvFTD patients. (a) Discriminant function consisted of GM ROI AD < controls; hippocampal volume; volume of putamen; FA ROI AD < controls; FA ROI bvFTD < controls; center; age; and sex. (b) Discriminant function consisted of GM ROI AD < controls; GM bvFTD < AD; L1 ROI AD > controls; L1 ROI bvFTD > controls; and L1 ROI bvFTD > AD. Blue squares indicate individual data of healthy controls, green dots indicate data of individual AD patients, red triangles indicate individual data of bvFTD patients. The black squares represent the group centroids.

The novelty of the study lies in the combination of three measures to separate AD from bvFTD. We combined VBM based measures of cortical atrophy, FIRST based measures of atrophy of DGM structures and DTI based measures of WM integrity to yield an optimal classifier.

**Table 4**
Structure matrix showing the discriminant loadings for each predictor. The structure matrix correlation coefficient represents the relative contribution of each predictor to group separation. (a) Discriminant analysis with GM ROIs, DGM structures and FA ROIs. (b) Discriminant analysis with GM ROIs, DGM structures and L1 and L23 ROIs.

| (a) | Function | |
|---|---|---|
| | 1 | 2 |
| GM ROI AD<Controls | ***0.469*** | ***0.449*** |
| Hippocampus | 0.222 | ***0.475*** |
| Putamen | 0.111 | 0.282 |
| FA ROI AD<Controls | 0.232 | ***0.451*** |
| FA ROI bvFTD<Controls | 0.131 | ***0.476*** |
| Center | -0.021 | -0.103 |
| Age | 0.187 | 0.111 |
| Sex | 0.003 | -0.121 |
| (b) | Function | |
| | 1 | 2 |
| GM ROI AD<Controls | ***0.642*** | ***0.400*** |
| GM ROI bvFTD<AD | 0.039 | ***0.706*** |
| L1 ROI bvFTD>AD | 0.026 | ***0.478*** |
| L1 ROI bvFTD>Controls | 0.183 | ***0.433*** |
| L1 ROI AD>Controls | 0.303 | ***0.329*** |

The values shown in this table are the structure matrix correlation coefficients, which are the correlations between the variable and the discriminant function. The discriminant function had a Wilk's lambda of 0.082 ($p \leq 0.001$). No specific p-values for the structure matrix correlation coefficients are given.

Both discriminant analyses revealed that cortical GM contributed to the separation of AD from the other two groups and WM integrity measurements contributed to the discrimination of bvFTD from the other groups. Especially axial diffusivity increased the discriminatory power for bvFTD. This could be explained by the notion that, despite some involvement of DGM and WM, AD is assumed to be a cortical dementia with specific GM regions being affected whereas bvFTD predominantly affect areas (frontal-insula-anterior cingulate) which are part of structurally and functionally connected neural networks. These networks are connected by specific WM tracts located within damaged GM areas as the frontal lobes and are preferentially affected, contributing to network failure in bvFTD. The finding of more severe damage of DGM structures add up to the hypotheses of bvFTD being a network disorder as DGM structures can be seen as relay stations in the fronto-striatal brain networks. These findings are further supported by the fact that bvFTD had the same disease stage (comparable MMSE, CDR, duration of symptoms) as AD patients but have more WM and DGM structure damage.

A possible limitation of this study is that we did not have post-mortem data available, so the possibility of misdiagnosis cannot be excluded. Nevertheless, we used an extensive standardized work-up and all AD patients fulfilled clinical criteria of probable AD, 19 patients fulfilled the criteria for probable bvFTD and 5 patients for possible bvFTD. All diagnoses were re-evaluated in a panel including clinicians from both centers to minimize sample effects. Because this is a multicenter study, the differences in data acquisition parameters between the two centers might introduce some noise in the DTI analysis. However, we adjusted for center in all models and moreover, a recent study showed that when considering scanner effects in the statistical model, no relevant differences between scanners were found (Teipel et al., 2012). To be confident that the different scanners did not essentially influence the results, we repeated the TBSS analyses for a subtest of all subjects of VUMC only and results remained essentially unchanged. Another limitation could be the significant age difference between the AD patients and controls. However, we corrected for age in all analyses and repeated the VBM, FIRST and TBSS analyses in an age matched subgroup which did not change the results essentially. Among the strengths of this study is the sample size and its multi-center nature. Most of the studies comparing AD with bvFTD use smaller sample sizes. We had enough power to detect differences using FWE and FWE-TFCE correction to adjust for multiple comparisons. Another strength is the unique combination of three imaging parameters in this study to achieve optimal discrimination between AD and bvFTD.

## 5. Conclusion

Accurate diagnosis of patients in life is increasingly important, both on clinical and scientific grounds. It is a guide to prognosis and prerequisite for optimal clinical care and management. AD and bvFTD are difficult to discriminate due to overlapping clinical and imaging features. Therefore, there is an urgent need to improve diagnostic accuracy in a quantitative manner. This study has shown that DTI measures add complementary information to measures of cortical and subcortical atrophy, thereby allowing a more precise diagnosis between AD and bvFTD. If acquisition, preprocessing and analyses methods are easier to implement in the daily clinical routine, DTI could be incorporated in the standard dementia MRI protocol in the future.

## Acknowledgements/disclosures

The VUMC Alzheimer Center is supported by Alzheimer Nederland and Stichting VUMC Fonds. Research of the VUMC Alzheimer Center is part of the neurodegeneration research program of the Neuroscience Campus Amsterdam. The clinical database structure was developed with funding from Stichting Dioraphte. This project is funded by the Netherlands Initiative Brain and Cognition (NIHC), a part of the Netherlands Organization for Scientific Research (NWO) under grant numbers 056-13-014 and 056-13-010. The gradient non-linearity correction was kindly provided by GE medical systems, Milwaukee.

Christiane Möller is appointed on a grant from the national project 'Brain and Cognition' ("Functionele Markers voor Cognitieve Stoornissen" (# 056-13-014)). She also received financial support from Alzheimer Nederland for attending courses.

Anne Hafkemeijer is appointed on a grant from the national project 'Brain and Cognition' ("Functionele Markers voor Cognitieve Stoornissen" (# 056-13-010)).

Dr. Yolande Pijnenburg reports no disclosures.

Prof. Dr. Serge Rombouts is supported by The Netherlands Organisation for Scientific Research (NWO), Vici project nr. 016.130.677.

Dr. Jeroen van der Grond reports no disclosures.

Elise Dopper reports no disclosures.

Prof. Dr. John van Swieten reports no disclosures.

Adriaan Versteeg reports no disclosures.

Dr. Petra Pouwels reports no disclosures.

Prof. Dr. Frederik Barkhof serves/has served on the advisory boards of: Bayer Schering Pharma, Sanofi-Aventis, Biogen Idec, UCB, Merck Serono, Novartis and Roche. He received funding from the Dutch MS Society and has been a speaker at symposia organized by the Serono Symposia Foundation. For all his activities he receives no personal compensation.

Prof. Dr. Philip Scheltens serves/has served on the advisory boards of: Genentech, Novartis, Roche, Danone, Nutricia, Baxter and Lundbeck. He has been a speaker at symposia organized by Lundbeck, Merz, Danone, Novartis, Roche and Genentech. He serves on the editorial board of Alzheimer's Research & Therapy and Alzheimer's Disease and Associated Disorders, is a member of the scientific advisory board of the EU Joint Programming Initiative and the French National Plan Alzheimer. For all his activities he receives no personal compensation.

Dr. Hugo Vrenken has received research support from Merck Serono, Novartis, and Pfizer, and speaker honoraria from Novartis; all funds were paid to his institution.

Dr. Wiesje van der Flier is recipient of The Alzheimer Nederland grant (Influence of age on the endophenotype of AD on MRI, project number 2010-002).

## Appendix A. Supplementary data

Supplementary data to this article can be found online at http://dx.doi.org/10.1016/j.nicl.2015.08.022.

## References


Agosta, F., Pievani, M., Sala, S., Geroldi, C., Galluzzi, S., Frisoni, G.B., et al., 2011. White matter damage in Alzheimer disease and its relationship to gray matter atrophy. Radiology 258 (3), 853–863. http://dx.doi.org/10.1148/radiol.1010128421177393.

Avants, B.B., Cook, P.A., Ungar, L., Gee, J.C., Grossman, M., 2010. Dementia induces correlated reductions in white matter integrity and cortical thickness: a multivariate neuroimaging study with sparse canonical correlation analysis. Neuroimage 50 (3), 1004–1016. http://dx.doi.org/10.1016/j.neuroimage.2010.01.04120083207.

Barnes, J., Whitwell, J.L., Frost, C., Josephs, K.A., Rossor, M., Fox, N.C., 2006. Measurements of the amygdala and hippocampus in pathologically confirmed Alzheimer disease and frontotemporal lobar degeneration. Arch. Neurol. 63 (10), 1434–1439. http://dx.doi.org/10.1001/archneur.63.10.143417030660.

Borroni, B., Brambati, S.M., Agosti, C., Gipponi, S., Bellelli, G., Gasparotti, R., et al., 2007. Evidence of white matter changes on diffusion tensor imaging in frontotemporal dementia. Arch. Neurol. 64 (2), 246–251. http://dx.doi.org/10.1001/archneur.64.2.24617296841.

Chen, T.F., Lin, C.C., Chen, Y.F., Liu, H.M., Hua, M.S., Huang, Y.C., et al., 2009. Diffusion tensor changes in patients with amnesic mild cognitive impairment and various dementias. Psychiatry Res. 173 (1), 15–21. http://dx.doi.org/10.1016/j.pscychresns.2008.09.00219442496.

Couto, B., Manes, F., Montañés, P., Matallana, D., Reyes, P., Velasquez, M., et al., 2013. Structural neuroimaging of social cognition in progressive non-fluent aphasia and behavioral variant of frontotemporal dementia. Front. Hum. Neurosci. 7, 467. http://dx.doi.org/10.3389/fnhum.2013.0046723966929.

Du, A.T., Schuff, N., Kramer, J.H., Rosen, H.J., Gorno-Tempini, M.L., Rankin, K., et al., 2007. Different regional patterns of cortical thinning in Alzheimer's disease and frontotemporal dementia. Brain 130 (4), 1159–1166. http://dx.doi.org/10.1093/brain/awm01617353226.

Filippi, M., Agosta, F., Scola, E., Canu, E., Magnani, G., Marcone, A., et al., 2013. Functional network connectivity in the behavioral variant of frontotemporal dementia. Cortex 49 (9), 2389–2401. http://dx.doi.org/10.1016/j.cortex.2012.09.01723164495.

Frisoni, G.B., Testa, C., Zorzan, A., Sabattoli, F., Beltramello, A., Soininen, H., et al., 2002. Detection of grey matter loss in mild Alzheimer's disease with voxel based morphometry. J. Neurol. Neurosurg. Psychiatry 73 (6), 657–664. http://dx.doi.org/10.1136/jnnp.73.6.65712438466.

Greicius, M.D., Geschwind, M.D., Miller, B.L., 2002. Presenile dementia syndromes: an update on taxonomy and diagnosis. J. Neurol. Neurosurg. Psychiatry 72 (6), 691–700. http://dx.doi.org/10.1136/jnnp.72.6.69112023408.

Halabi, C., Halabi, A., Dean, D.L., Wang, P.N., Boxer, A.L., Trojanowski, J.Q., et al., 2013. Patterns of striatal degeneration in frontotemporal dementia. Alzheimer Dis. Assoc. Disord. 27 (1), 74–83. http://dx.doi.org/10.1097/WAD.0b013e31824a7df4.

Harris, J.M., Thompson, J.C., Gall, C., Richardson, A.M., Neary, D., du Plessis, D., et al., 2015. Do NIA-AA criteria distinguish Alzheimer's disease from frontotemporal dementia? Alzheimers Dement 11 (2), 207–215. http://dx.doi.org/10.1016/j.jalz.2014.04.51625022535.

Harvey, R.J., Skelton-Robinson, M., Rossor, M.N., 2003. The prevalence and causes of dementia in people under the age of 65 years. J. Neurol. Neurosurg. Psychiatry 74 (9), 1206–1209. http://dx.doi.org/10.1136/jnnp.74.9.120612933919.

Hornberger, M., Geng, J., Hodges, J.R., 2011. Convergent grey and white matter evidence of orbitofrontal cortex changes related to disinhibition in behavioural variant frontotemporal dementia. Brain 134 (9), 2502–2512. http://dx.doi.org/10.1093/brain/awr17321785117.

Hornberger, M., Piguet, O., 2012. Episodic memory in frontotemporal dementia: a critical review. Brain 135 (3), 678–692. http://dx.doi.org/10.1093/brain/aws01122366790.

Hornberger, M., Piguet, O., Kipps, C., Hodges, J.R., 2008. Executive function in progressive and nonprogressive behavioral variant frontotemporal dementia. Neurology 71 (19), 1481–1488. http://dx.doi.org/10.1212/01.wnl.0000334299.72023.c818981369.

Jenkinson, M., Beckmann, C.F., Behrens, T.E.J., Woolrich, M.W., Smith, S.M., 2012. FSL. Neuroimage 62 (2), 782–790. http://dx.doi.org/10.1016/j.neuroimage.2011.09.015.

Kuceyeski, A., Zhang, Y., Raj, A., 2012. Linking white matter integrity loss to associated cortical regions using structural connectivity information in Alzheimer's disease and fronto-temporal dementia: the loss in connectivity (loco) score. Neuroimage 61 (4), 1311–1323. http://dx.doi.org/10.1016/j.neuroimage.2012.03.03922484307.

Looi, J.C., Lindberg, O., Zandbelt, B.B., Ostberg, P., Andersen, C., Botes, L., et al., 2008. Caudate nucleus volumes in frontotemporal lobar degeneration: differential atrophy in subtypes. A.J.N.R. Am. J. Neuroradiol. 29 (8), 1537–1543. http://dx.doi.org/10.3174/ajnr.A116818782907.

Looi, J.C., Svensson, L., Lindberg, O., Zandbelt, B.B., Ostberg, P., Orndahl, E., et al., 2009. Putaminal volume in frontotemporal lobar degeneration and Alzheimer disease: differential volumes in dementia subtypes and controls. A.J.N.R. Am. J. Neuroradiol. 30 (8), 1552–1560. http://dx.doi.org/10.3174/ajnr.A164019497964.

Looi, J.C., Walterfang, M., Velakoulis, D., Macfarlane, M.D., Svensson, L.A., Wahlund, L.O., 2012. Frontotemporal dementia as a frontostriatal disorder: neostriatal morphology as a biomarker and structural basis for an endophenotype. Aust. N. Z. J. Psychiatry 46 (5), 422–434. http://dx.doi.org/10.1177/0004867411432076225352922.

Mahoney, C.J., Ridgway, G.R., Malone, I.B., Downey, L.E., Beck, J., Kinnunen, K.M., et al., 2014. Profiles of white matter tract pathology in frontotemporal dementia. Hum. Brain Mapp. 35 (8), 4163–4179. http://dx.doi.org/10.1002/hbm.2246824510641.

Matsuo, K., Mizuno, T., Yamada, K., Akazawa, K., Kasai, T., Kondo, M., et al., 2008. Cerebral white matter damage in frontotemporal dementia assessed by diffusion tensor tractography. Neuroradiology 50 (7), 605–611. http://dx.doi.org/10.1007/s00234-008-0379-518379765.

McKhann, G., Drachman, D., Folstein, M., Katzman, R., Price, D., Stadlan, E.M., 1984. Clinical diagnosis of Alzheimer's disease: report of the NINCDS-ADRDA Work Group under the auspices of Department of Health and Human Services Task Force on Alzheimer's Disease. Neurol. 34 (7), 939–944. http://dx.doi.org/10.1212/WNL.34.7.9396610841.

McKhann, G.M., Knopman, D.S., Chertkow, H., Hyman, B.T., Jack Jr., C.R., Kawas, C.H., et al., 2011. The diagnosis of dementia due to Alzheimer's disease: recommendations from the National Institute on Aging–Alzheimer's Association workgroups on diagnostic guidelines for Alzheimer's disease. Alzheimer's & Dementia 7 (3), 263–269. http://dx.doi.org/10.1016/j.jalz.2011.03.005.

McMillan, C.T., Brun, C., Siddiqui, S., Churgin, M., Libon, D., Yushkevich, P., et al., 2012. White matter imaging contributes to the multimodal diagnosis of frontotemporal lobar degeneration. Neurology 78 (22), 1761–1768. http://dx.doi.org/10.1212/WNL.0b013e31825830bd22592372.

Miller, B.L., Diehl, J., Freedman, M., Kertesz, A., Mendez, M., Rascovsky, K., 2003. International approaches to frontotemporal dementia diagnosis: from social cognition to neuropsychology. Ann. Neurol. 54 (Suppl. 5), S7–10. http://dx.doi.org/10.1002/ana.1056812833361.

Möller, C., Vrenken, H., Jiskoot, L., Versteeg, A., Barkhof, F., Scheltens, P., et al., 2013. Different patterns of gray matter atrophy in early- and late-onset Alzheimer's disease. Neurobiol. Aging 34 (8), 2014–2022. http://dx.doi.org/10.1016/j.neurobiolaging.2013.02.013.

Muñoz-Ruiz, M.Á, Hartikainen, P., Koikkalainen, J., Wolz, R., Julkunen, V., Niskanen, E., et al., 2012. Structural MRI in frontotemporal dementia: comparisons between hippocampal volumetry, tensor-based morphometry and voxel-based morphometry. PLOS ONE 7 (12), e52531. http://dx.doi.org/10.1371/journal.pone.005253123285078.

Nestor, P.J., Scheltens, P., Hodges, J.R., 2004. Advances in the early detection of Alzheimer's disease. Nat. Med. 10 (Suppl.), S34–S41. http://dx.doi.org/10.1038/nrn143315298007.

Patenaude, B., Smith, S.M., Kennedy, D.N., Jenkinson, M., 2011. A Bayesian model of shape and appearance for subcortical brain segmentation. Neuroimage 56 (3), 907–922. http://dx.doi.org/10.1016/j.neuroimage.2011.02.04621352927.

Popescu, V., Battaglini, M., Hoogstrate, W.S., Verfaillie, S.C., Sluimer, I.C., van Schijndel, R.A., et al., 2012. Optimizing parameter choice for FSL-Brain Extraction Tool (BET) on 3D T1 images in multiple sclerosis. Neuroimage 61 (4), 1484–1494. http://dx.doi.org/10.1016/j.neuroimage.2012.03.07422484407.

Rabinovici, G.D., Miller, B.L., 2010. Frontotemporal lobar degeneration. CNS Drugs 24 (5), 375–398. http://dx.doi.org/10.2165/11533100-000000000-00000.

Rabinovici, G.D., Seeley, W.W., Kim, E.J., Gorno-Tempini, M.L., Rascovsky, K., Pagliaro, T.A., et al., 2007. Distinct MRI atrophy patterns in autopsy-proven Alzheimer's disease and frontotemporal lobar degeneration. Am J Alzheimers Dis Other Demen 22 (6), 474–488. http://dx.doi.org/10.1177/1533317507308779181666607.

Rascovsky, K., Hodges, J.R., Knopman, D., Mendez, M.F., Kramer, J.H., Neuhaus, J., et al., 2011. Sensitivity of revised diagnostic criteria for the behavioural variant of frontotemporal dementia. Brain 134 (9), 2456–2477. http://dx.doi.org/10.1093/brain/awr17921810890.

Ratnavalli, E., Brayne, C., Dawson, K., Hodges, J.R., 2002. The prevalence of frontotemporal dementia. Neurology 58 (11), 1615–1621. http://dx.doi.org/10.1212/WNL.58.11.1615.

Salat, D.H., Tuch, D.S., van der Kouwe, A.J.W., Greve, D.N., Pappu, V., Lee, S.Y., et al., 2010. White matter pathology isolates the hippocampal formation in Alzheimer's disease. Neurobiol. Aging 31 (2), 244–256. http://dx.doi.org/10.1016/j.neurobiolaging.2008.03.013.

Scola, E., Bozzali, M., Agosta, F., Magnani, G., Franceschi, M., Sormani, M.P., et al., 2010. A diffusion tensor MRI study of patients with MCI and AD with a 2-year clinical follow-up. J. Neurol. Neurosurg. Psychiatry 81 (7), 798–805. http://dx.doi.org/10.1136/jnnp.2009.189639.

Smith, S.M., Jenkinson, M., Johansen-Berg, H., Rueckert, D., Nichols, T.E., Mackay, C.E., et al., 2006. Tract-based spatial statistics: voxelwise analysis of multi-subject diffusion data. Neuroimage 31 (4), 1487–1505. http://dx.doi.org/10.1016/j.neuroimage.2006.02.024.

Smith, S.M., Jenkinson, M., Woolrich, M.W., Beckmann, C.F., Behrens, T.E.J., Johansen-Berg, H., et al., 2004. Advances in functional and structural MR image analysis and implementation as FSL. Neuroimage 23, S208–S219. http://dx.doi.org/10.1016/j.neuroimage.2004.07.051.

Smith, S.M., Zhang, Y., Jenkinson, M., Chen, J., Matthews, P.M., Federico, A., et al., 2002. Accurate, robust, and automated longitudinal and cross-sectional brain change analysis. Neuroimage 17 (1), 479–489. http://dx.doi.org/10.1006/nimg.2002.1040.

Smits, L., Pijnenburg, Y., Koedam, E., van der Vlies, A., Roos-Reuling, I., Koene, T., et al., 2011. Early-onset Alzheimer's disease is associated with a distinct neuropsychological profile. Alzheimer's & Dementia 7 (4). http://dx.doi.org/10.1016/j.jalz.2011.05.760.

Teipel, S.J., Wegrzyn, M., Meindl, T., Frisoni, G., Bokde, A.L., Fellgiebel, A., et al., 2012. Anatomical MRI and DTI in the diagnosis of Alzheimer's disease: a European multicenter study. J. Alzheimers Dis. 31 (Suppl. 3), S33–S47. http://dx.doi.org/10.3233/JAD-2012-11211822992380.

van de Pol, L.A., Hensel, A., van der Flier, W.M., Visser, P.J., Pijnenburg, Y.A., Barkhof, F., et al., 2006. Hippocampal atrophy on MRI in frontotemporal lobar degeneration and Alzheimer's disease. J. Neurol. Neurosurg. Psychiatry 77 (4), 439–442. http://dx.doi.org/10.1136/jnnp.2005.075341.

Verhage, F., 1964. Intelligentie en leeftijd: onderzoek bij Nederlanders van twaalf tot zevenenzeventig jaar. van Gorcum, Assen.

Walker, A.J., Meares, S., Sachdev, P.S., Brodaty, H., 2005. The differentiation of mild frontotemporal dementia from Alzheimer's disease and healthy aging by neuropsychological tests. Int. Psychogeriatr. 17 (1), 57–68. http://dx.doi.org/10.1017/S1041610204000778.

Whitwell, J.L., Jack Jr., C.R., Przybelski, S.A., Parisi, J.E., Senjem, M.L., Boeve, B.F., et al., 2011. Temporoparietal atrophy: a marker of AD pathology independent of clinical diagnosis. Neurobiol. Aging 32 (9), 1531–1541. http://dx.doi.org/10.1016/j.neurobiolaging.2009.10.012.

Zhang, Y., Brady, M., Smith, S., 2001. Segmentation of brain MR images through a hidden Markov random field model and the expectation-maximization algorithm. I.E.E.E. Trans. Med. Imaging 20 (1), 45–57. http://dx.doi.org/10.1109/42.906424.

Zhang, Y., Schuff, N., Ching, C., Tosun, D., Zhan, W., Nezamzadeh, M., et al., 2011. Joint assessment of structural, perfusion, and diffusion MRI in Alzheimer's disease and frontotemporal dementia. Int. J. Alzheimers Dis 2011, 1–11. http://dx.doi.org/10.4061/2011/546871.

Zhang, Y., Schuff, N., Du, A.-T., Rosen, H.J., Kramer, J.H., Gorno-Tempini, M.L., et al., 2009. White matter damage in frontotemporal dementia and Alzheimer's disease measured by diffusion MRI. Brain 132 (9), 2579–2592. http://dx.doi.org/10.1093/brain/awp071.

Zhou, J., Greicius, M.D., Gennatas, E.D., Growdon, M.E., Jang, J.Y., Rabinovici, G.D., et al., 2010. Divergent network connectivity changes in behavioural variant frontotemporal dementia and Alzheimer's disease. Brain 133 (5), 1352–1367. http://dx.doi.org/10.1093/brain/awq075.